

Effect of hydrostatic pressure on the direct absorption edge of germanium

Benjamin Welber and Manuel Cardona*

IBM Thomas J. Watson Research Center, Yorktown Heights, New York 10598

Yet-Ful Tsay and Bernard Bendow

Solid State Science Division, Deputy for Electronic Technology, RADC, Hanscom AFB, Massachusetts 01731

(Received 2 September 1976)

The dependence of the direct gap of germanium ($\Gamma_{25'} \rightarrow \Gamma_2$) on hydrostatic pressures up to 104 kbar has been measured. This dependence is found to be sublinear and to reflect mostly the nonlinearity in the compressibility. The linear pressure coefficient found for the gap is $(1.53 \pm 0.05) \times 10^{-2}$ eV/kbar while the quadratic one amounts to $-(4.5 \pm 1) \times 10^{-5}$ eV/kbar². When the gap is plotted as a function of lattice constant a small sublinearity remains. This sublinearity is well reproduced by a calculation based on empirical pseudopotential coefficients. At pressures above 8 kbars a strong tail develops below the direct edge. It is attributed to $\Gamma_{25'} \rightarrow L_1$ and $\Gamma_{25'} \rightarrow \Delta_1$ indirect transitions. The strength of the direct exciton edge is found to evolve with pressure in a way proportional to the $\Gamma_{25'} \rightarrow \Gamma_2$ gap energy. At 105 kbar the material is found to become opaque as a result of a phase transition.

I. INTRODUCTION

The development of the diamond anvil cell and the ruby fluorescence manometer¹ has made possible optical measurements under pure hydrostatic pressures in excess of 100 kbar.^{2,3} A study of the direct edge of GaAs ($\Gamma_{15} \rightarrow \Gamma_1$, also referred to as E_0) for pressures up to the phase transition (180 kbar) has revealed a sublinear variation of the gap energy with pressure.³ Most of this nonlinearity is related to nonlinearities in the bulk modulus: it disappears when the gap is plotted as a function of lattice constant. However, a small sublinearity remains in the dependence of the E_0 gap of GaAs on lattice constant. This sublinearity can be theoretically explained with the empirical dielectric theory of energy gaps^{3,4} and with the empirical pseudopotential method.⁵ A calculation based on Heine and Cohen analytic pseudopotentials gives a superlinear pressure dependence of E_0 unless pressure-dependent hard-core pseudopotential radii are assumed.³

As a result of the sublinearity in the pressure dependence of E_0 , the linear pressure coefficients found in conventional measurements, limited to pressures below 10 kbar (1.1×10^{-2} eV/kbar for GaAs), are too low. Nonlinearities may also be responsible for the wide range of pressure coefficients reported for the E_0 edge⁶ of Ge (between 1.1 and 1.4×10^{-2} eV/kbar) while significantly higher values have been calculated⁷ (1.6×10^{-2} eV/kbar). In order to test this idea and to clarify the origin of these nonlinearities we have performed measurements of the pressure dependence of the E_0 gap of Ge up to the phase transition (105 kbar). We found a nonlinear behavior similar to that found earlier for GaAs and

deduced an initial slope of 1.53 ± 0.05 eV/kbar, higher than any previously reported. The nonlinear behavior is reproduced by a calculation based on empirical pseudopotential coefficients.^{5,7} As a by-product, we have shown that the height of the exciton-induced step in the absorption coefficient is proportional to the gap energy, as required by Elliott's theory.⁸ Above 8 kbar a tail develops below the E_0 gap. This tail grows as the pressure is increased. A comparison with the indirect edges of Ge ($\Gamma_{25'} \rightarrow L_1$) and Si ($\Gamma_{25'} \rightarrow \Delta_1$) suggests that this tail is due to both types of indirect transitions, with a small contribution ($\sim 20\%$) of $\Gamma_{25'} \rightarrow \Delta_1$ via the Γ_2 intermediate state. This intermediate state should not contribute to the $\Gamma_{25'} \rightarrow \Delta_1$ transitions of Si since it occurs 4 eV above the $\Gamma_{25'}$ valence band.

II. EXPERIMENT AND RESULTS

The details of the optical and pressure apparatus have been published in Ref. 3. The sample was a $10\text{-}\mu\text{m}$ -thick piece of Ge measuring about 0.1 mm across. It was prepared by chemically etching a polished platelet of $10\ \Omega\ \text{cm}$ n -type Ge and by cracking it into small pieces. The pressure was measured to within ± 1 kbar by using the shift of the fluorescence lines of a small piece of ruby placed in the pressure cell.¹ All measurements were performed at room temperature.

While Ge has an indirect edge ($\Gamma_{25'} \rightarrow L_1$) at 0.65 eV at room temperature, the absorption near this edge is weak and the direct edge ($\Gamma_{25'} \rightarrow \Gamma_2$) appears strongly as a sharp excitonic step^{8,9} which saturates at 0.82 eV at atmospheric pressure (see Fig. 1). We take this saturation point or kink

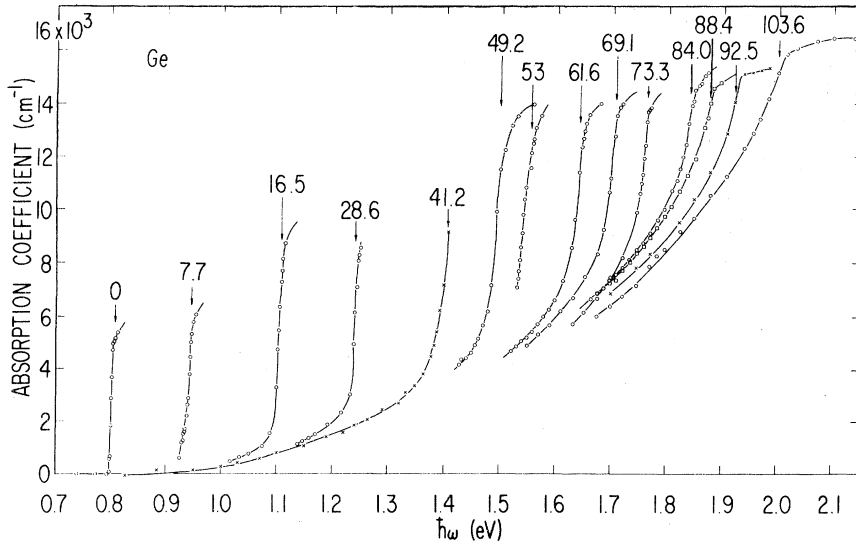


FIG. 1. Absorption edges of Ge obtained at room temperature and for several hydrostatic pressures up to the phase transitions. The vertical values indicate the position of the excitonic "kink" as obtained from the transmission curves. The numbers on the vertical arrows represent the pressure (in kbar) at which the data were taken.

as indicated by the arrows of Fig. 1, to be the direct gap since, within the accuracy of the room-temperature measurements, the excitonic binding energy¹⁰ (0.002 eV) can be neglected. This kink is better defined in the transmission curves (I/I_0) than in the absorption coefficient $\alpha = -(1/d)\ln(I/I_0)$ and we usually took it from the transmission curves. The energy of the direct gap obtained in this manner is plotted in Fig. 2 as a function of pressure p . The strong nonlinearity in the $E_0(p)$ curve is similar to that reported for GaAs.³ A quadratic least-square fit to the experimental points yields for the linear and quadratic pressure

coefficients

$$\frac{dE_0}{dp} = (1.53 \pm 0.05) \times 10^{-2} \text{ eV/kbar},$$

$$\frac{1}{2} \frac{d^2E_0}{dp^2} = -(4.5 \pm 1) \times 10^{-5} \text{ eV/kbar}^2.$$

III. DISCUSSION

It has been shown recently⁵ that the pressure dependence of the E_0 gap of GaAs measured up to 180 kbar can be accounted rather well by band-structure calculations as a function of lattice constant based on the empirical pseudopotential method.⁷ We present here the results of similar calculations for Ge. The ionic pseudopotential form factors (PFF) are obtained as a function of wave vector \vec{q} by fitting a second-degree polynomial to the symmetric crystal PFF of Ge given by Cohen and Bergstresser,¹¹ after multiplication by the volume of the unit cell and the q -dependent dielectric constant. This dielectric constant $\epsilon^*(q)$ is taken to be that of the Penn model suitably modified by Brust to include exchange and correlation.⁷ The q -dependent crystal PFF of Ge are then obtained by dividing the ionic PFF by the volume of the unit cell (dependent on lattice constant) and by $\epsilon^*(q)$. This involves the use of a self-consistency loop since $\epsilon^*(q)$ is a function of the average (Penn) gap, which is taken to the gap calculated for the $(2\pi/a)(\frac{1}{2}, \frac{1}{2}, 0)$ point of the Brillouin zone. The band structure was obtained by diagonalizing a secular equation with approximately 20 rows (15 at the Γ point and 22 at the L point) with about 80 additional waves included by Löwdin perturbation theory.

The dependence of the E_0 direct gap and of the

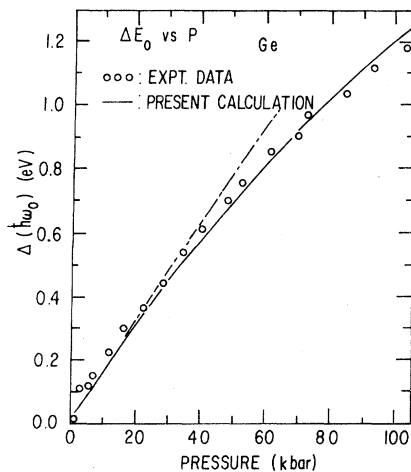


FIG. 2. Direct energy gap of Ge vs pressure at room temperature (circles). The solid line represents the pseudopotential calculations discussed in Sec. III, while the dashed line represents the initial slope of the quadratic fit to the experimental points.

$\Gamma_{25'} \rightarrow L_1$ indirect gap (E_i) on lattice constant calculated by this procedure is shown in Fig. 3. The gaps obtained for the zero-pressure lattice constant a_0 ($\Delta a = 0$) are somewhat larger than the experimental ones, a result due, in part, to having neglected the spin-orbit splitting in the calculation (the spin-orbit splitting decreases both gaps by 0.1 eV) and to the fact that no parameters were adjusted by ourselves. The three PFF of Cohen and Bergstresser were adjusted so as to optimize the agreement with seven energy gaps measured at low temperature. The two gaps of Fig. 3 for $\Delta a = 0$ appear in a pseudopotential calculation as the difference of two large energies and are therefore rather sensitive to the value of the PFF chosen. This is, however, not the case for their pressure coefficients.¹²

The calculated gaps of Fig. 3 are seen to vary nearly linearly with $\Delta a/a_0$. However, a slight sublinearity can be detected. The variation of E_0 and E_i with $\Delta a/a_0$ is represented by

$$\begin{aligned} \Delta E_0(\text{eV}) &= -37.5 (\Delta a/a_0) - 52 (\Delta a/a_0)^2, \\ \Delta E_i(\text{eV}) &= -19(\Delta a/a_0) - 65(\Delta a/a_0)^2. \end{aligned} \quad (1)$$

In order to compare our calculations with the experimental results, we used Murnaghan's equation of state¹³

$$p = (B_0/B'_0)[(a_0/a)^{3B'_0} - 1], \quad (2)$$

where a is the lattice constant under a pressure p , B_0 the bulk modulus¹⁴ ($B_0 = 743.7$ kbar), and B'_0 its pressure derivative¹⁴ (4.76). The theoretical dependence of Fig. 3, converted into a function of

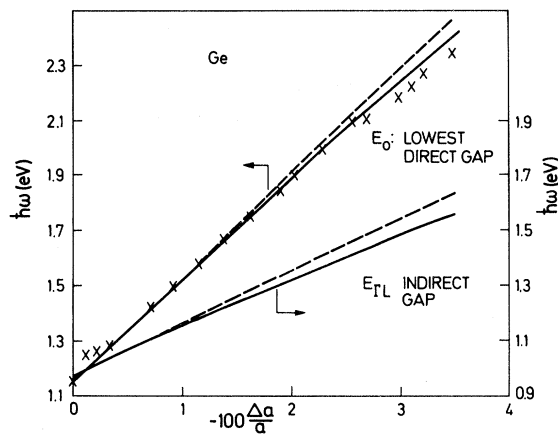


FIG. 3. Calculated dependence on lattice constant of the E_0 direct gap (solid lines) and the $\Gamma_{25'} \rightarrow L_1$ indirect gap of Ge. The dashed line indicates the initial slopes of the calculated curves. The crosses represent our experimental data for the E_0 edge with the origin of energies shifted to make comparison with calculations possible.

p with Eq. (2), is represented by the solid line of Fig. 2. Practically the same line is obtained with Birch's equation of state.¹⁵ It fits the experimental points rather well except maybe for the two highest pressures. A glance at Fig. 1, however, shows that at these pressures the edge is broadened, becomes less well defined, and may even be lowered by interaction with the large background of indirect transitions. The large absorption coefficients used may also produce an apparent lowering of the edge due to scattered light. One should also point out that a calculation using the analytic atomic PFF of Cohen and Heine¹⁶ yielded a slightly superlinear dependence of E_0 on $\Delta a/a_0$ instead of the sublinear ones of Fig. 3. We have also plotted in Fig. 3 the observed energy gaps E_0 with the pressure transformed into lattice constants using Eq. (2) (a constant has been added to the E_0 energies to make comparison with the calculations possible). A slight sublinearity, similar to the calculated one, is apparent in the experimental points. We point out that a plot of the experimental points as function of volume shows a larger, well defined sublinearity.

For pressures above 8 kbars a tail develops below the E_0 excitonic step. This tail must be due to indirect transitions from $\Gamma_{25'}$ to the L_1 and the Δ_1 conduction minima ($E_i = 0.65$ and 0.86 eV, respectively, at¹⁷ $T = 300$ K and $p = 0$). Experiments with thicker samples (≥ 0.1 mm) should yield the pressure dependence of these indirect edges which could then be compared to the calculations of Fig. 3 for the $\Gamma_{25'} \rightarrow L_1$ edge and to similar calculations for the $\Gamma_{25'} \rightarrow \Delta_1$ edge. The pressure coefficient obtained from Eq. (1) and B_0 for the $\Gamma_{25'} \rightarrow L$ edge is 8×10^{-3} eV/kbar, considerably larger than the experimental value^{18, 19} (5×10^{-3} eV/kbar). The pressure coefficient of the $\Gamma_{25'} \rightarrow \Delta_1$ edge of Si has been measured up to 7 kbars and equals -10^{-3} eV/kbar.¹⁸ The calculations of Ref. 5 yield a positive coefficient at zero pressure which reverses sign at higher pressures: large errors are, however, expected in the calculations of such small coefficients which arise from compensating terms. For this reason we have not included in Fig. 3 the pressure dependence of the $\Gamma_{25'} \rightarrow \Delta_1$ gap.

We shall now try to analyze the indirect tail of the 41.2-kbars curve of Fig. 1 (replotted as the crosses of Fig. 4), for which the most detailed data were taken. The absorption coefficient for allowed phonon induced indirect transitions between parabolic bands can be written¹⁸

$$\alpha = A \sum_j \frac{P_j^2 (m_c m_v)^{3/2} \Xi_{ep,i}^2 (2n_B + 1)}{\omega n \langle |\Delta\omega|^2 \rangle} (\omega - \omega_i)^2, \quad (3)$$

where P_j is the matrix element of linear momentum between initial and intermediate state j or be-

tween intermediate and final state (dependent on order of phonon and photon transitions), m_c and m_v are the effective masses of the initial and final bands, respectively, $\Xi_{ep,i}$ is the corresponding matrix element of the electron-phonon interaction, ω_i the indirect gap (the phonon energies are being neglected since in our measurements the edge cannot be decomposed into its phonon absorption and emission components), n_B the Bose-Einstein statistical factor for the appropriate phonon, n the refractive index (nearly constant in the region of interest), and $\langle |\Delta\omega|^2 \rangle^{1/2}$ an average energy difference between the intermediate and the final state. The contribution of the $\Gamma_{25'} \rightarrow L_1$ indirect transitions to Fig. 4 can be estimated by extrapolation of the corresponding transitions observed at zero pressure. We find from Refs. 18–20

$$\alpha = 6.25 \times 10^3 (\omega - 0.65)^2 \text{ cm}^{-1}, \quad (4)$$

with ω in eV. A comparison of Eq. (4) with Eq. (3) indicates that there must be a cancellation in the ω dependence of terms ω and $\langle |\Delta\omega|^2 \rangle$ in the denominator of Eq. (3) which may be also helped by a frequency dependence of the terms in the numerator, such as $P_x \Xi_{ep,i}$. The simple form of Eq. (4) suggests an estimate of the contribution of the $\Gamma_{25'} \rightarrow L_1$ transitions to the indirect absorption of Fig. 4 merely by shifting ω_i from 0.65 to 0.93 eV, the value calculated at 4.12 kbar with the help of Fig. 3. This gives the dashed line of Fig. 4 which is obviously insufficient to account for the observed absorption. The reason is to be sought in the contribution of $\Gamma_{25'} \rightarrow \Delta_1$ transitions which can be estimated from the indirect edge of Si. In fact, all of the band parameters which contribute to the $\Gamma_{25'} \rightarrow \Delta_1$ transitions should be nearly

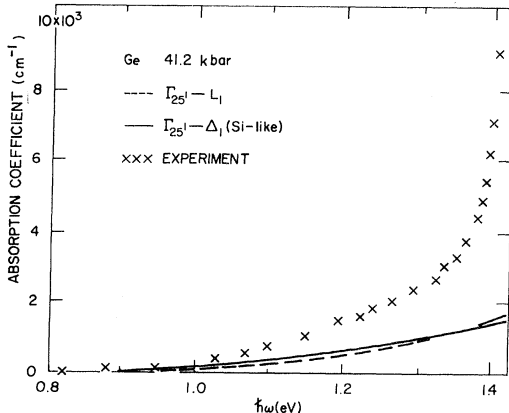


FIG. 4. Experimental absorption edge of Ge at 41.2 kbars and 300 K (crosses). The dashed line represents the $\Gamma_{25'} \rightarrow L_1$ indirect transitions estimated on the basis of the indirect absorption edge of Ge. The solid line is an estimate of the $\Gamma_{25'} \rightarrow \Delta_1$ transitions based on the indirect edge of Si.

the same for Ge as for Si, with the exception of the presence in Ge of transitions via the Γ_2' intermediate state. This state is too far away in Si to contribute.²¹ For Si the $\Gamma_{25'} \rightarrow \Delta_1$ indirect absorption is

$$\alpha = 4 \times 10^3 (\omega - 1.06)^2 \text{ cm}^{-1}, \quad (5)$$

with ω in eV. In order to find the corresponding absorption coefficient of Ge at 41.2 kbar, the $\Gamma_{25'} \rightarrow \Delta_1$ gap of this material¹⁷ (0.86 eV) must be shifted down by about 0.04 eV as obtained from the pressure coefficient of this gap in Si.¹⁸ We also must take care of the different statistical factors n_B in Eq. (3) (the transitions occur mainly by absorption or emission of TO phonons²³ with energy 0.058 for Si and 0.036 for Ge). The statistical factor $2n_B + 1$ should enhance the absorption of Ge by a factor of 1.32 with respect to Si. Besides, the matrix element Ξ^2 is proportional to the square of the amplitude of the zero-point vibration, inversely proportional to the square root of the atomic mass. This introduces a factor $(M_{\text{Si}}/M_{\text{Ge}})^{1/2} = 0.62$. The factor of ω in the denominator of Eq. (3) suggests the multiplication of the absorption of Si by the ratio of the indirect gap of Si to the corresponding one of stressed Ge (1.06/0.82 = 1.3). Thus, from Eq. (4) and the above we find

$$\alpha = 4.2 \times 10^3 (\omega - 0.82)^2 \text{ cm}^{-1}, \quad (6)$$

with ω in eV. The sum of the two calculated curves of Fig. 4 accounts for about 80% of the observed indirect tail. The remaining 20%, although it falls in the range of the uncertainties involved in our estimates, could be due to $\Gamma_{25'} \rightarrow \Delta_1$ indirect transitions via the Γ_2' intermediate state. These transitions take place with participation of LO phonons, in contrast to the TO phonon aided Si-like transitions. Absorption studies of thicker samples near the indirect exciton threshold should be able to separate the contributions of the various phonons and thus to test our conjecture concerning the various intermediate states involved.

We discuss now the strength of the direct excitonic step of Fig. 1 and its pressure dependence. The strength of the excitonic step is given by (in a.u.)^{8, 12}

$$\Delta\alpha = (4\pi/c\omega_0 n) P_x^2 (2\mu)^{3/2} (E_{\text{ex}})^{1/2}, \quad (7)$$

where c is the speed of light, n the refractive index¹² (≈ 4.2), P_x the matrix element of linear momentum between valence and conduction bands (≈ 0.41 at units per each valence band¹²), μ the reduced density of states mass, and E_{ex} the exciton binding energy¹⁰ (1.7 meV) which is approximately equal to $\mu/2\epsilon$ a.u. ($\mu = 0.033$, $\epsilon = 16$). Replacement

of these values into Eq. (7) yields at zero pressure $\Delta\alpha = 3.1 \times 10^3 \text{ cm}^{-1}$. This value should be multiplied by two to take into account the degeneracy of the valence bands. One then obtains $\Delta\alpha = 6.2 \times 10^3 \text{ cm}^{-1}$, in excellent agreement with the zero-pressure data of Fig. 1.

It is easy to find an explicit expression for the dependence of $\Delta\alpha$ on pressure. This dependence arises mainly from the explicit ω_0 dependence in Eq. (7) and from the dependence of μ and E_{ex} on ω_0 . The dependence of the dielectric constant and of P on pressure can be neglected.¹² Replacing $E_x \propto \mu$ and $\mu \propto E_0/P_x^2$ in Eq. (7) we find that $\Delta\alpha$ should be *directly* proportional to ω_0 . The strength of the excitonic step, as measured from the indirect background, is plotted in Fig. 5 as a function of ω_0 . A linear dependence holds for ω_0 up to 1.5 eV (~ 50 kbars). Up to this pressure the steepness of the excitonic step does not change. At higher pressures, the step begins to broaden and becomes ill defined, probably because of decay into the large growing indirect background. At the highest pressures the broadened step can no longer be separated from the indirect transitions background.

In conclusion, we have measured the dependence of the energy of the direct gap of Ge on hydrostatic pressures up to 104 kbar and found it to be sublinear. While most of the sublinearity is due to the decrease in compressibility with increasing pressure, a small sublinearity remains when the gap is plotted as a function of lattice constant. This sublinearity is explained by an empirical pseudopotential calculation. With increasing

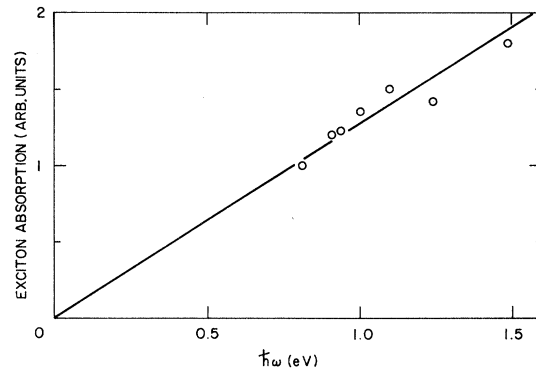


FIG. 5. Strength of the step in the absorption coefficient of Ge due to direct excitons, as a function of the direct gap energy which is varied by application of hydrostatic pressure.

pressure, strong indirect transitions ($\Gamma_{25'} \rightarrow L_1$ and $\Gamma_{25'} \rightarrow \Delta_1$) appear below the direct edge. Experiments with thicker samples should yield detailed information about these indirect transitions.

ACKNOWLEDGMENTS

We would like to thank Dr. C. K. Kim and Professor S. Rodriguez for valuable discussions and Dr. M. H. Brodsky for a critical reading of the manuscript. Thanks are also due to Dr. G. J. Piermarini and Dr. S. Black for their advice in high pressure technology, to Dr. J. Marinace for help with the sample preparation, and to Dr. R. J. Keyes for several stimulating conversations.

*Permanent Address: Max Planck Institut für Festkörperforschung, Stuttgart, Federal Republic of Germany.

¹J. D. Barnett, S. Block, and G. J. Piermarini, *Rev. Sci. Instrum.* **44**, 1 (1973); G. J. Piermarini, S. Block, and J. D. Barnett, *J. Appl. Phys.* **44**, 5377 (1973).
²B. A. Weinstein and G. Piermarini, *Phys. Rev.* **12**, 1172 (1975).
³B. Welber, M. Cardona, C. K. Kim, and S. Rodriguez, *Phys. Rev.* **12**, 5729 (1975).
⁴D. L. Camphausen, G. A. N. Connell, and W. Paul, *Phys. Rev. Lett.* **26**, 184 (1971).
⁵Y. F. Tsay and B. Bendow, *Phys. Rev.* (to be published).
⁶See, for instance, P. J. Melz, *J. Phys. Chem. Solids* **32**, 209 (1971).
⁷Y. F. Tsay, S. S. Mitra, and B. Bendow *Phys. Rev.* **10**, 1476 (1974).
⁸R. J. Elliott, *Phys. Rev.* **108**, 1384 (1957).
⁹W. C. Dash and R. Newman, *Phys. Rev.* **99**, 1151 (1955).
¹⁰B. Lax and S. Zwerdling in *Progress in Semiconductors*, edited by A. F. Gibson and R. E. Burgess (Temple, London, 1960), Vol. 5.
¹¹M. L. Cohen and T. K. Bergstresser, *Phys. Rev.* **141**,

789 (1966).

¹²M. Cardona in *Atomic Structure and Properties of Solids*, edited by E. Burstein (Academic, New York, 1972), p. 539.
¹³F. D. Murnaghan, *Proc. Natl. Acad. Sci. USA* **30**, 244 (1944).
¹⁴H. J. McSkimin, A. Jarayaman, and P. Andreatch, *J. Appl. Phys.* **38**, 2362 (1967).
¹⁵F. Birch, *Phys. Rev.* **71**, 809 (1947).
¹⁶C. K. Kim (private communication).
¹⁷R. Braunstein, A. R. Moore, and F. Herman, *Phys. Rev.* **109**, 695 (1958).
¹⁸W. Paul and D. M. Warshauer, *J. Phys. Chem. Solids* **5**, 89 (1958); **6** (1958).
¹⁹A. Jayaraman, B. B. Kosicki, and J. C. Irvin, *Phys. Rev.* **171**, 836 (1968).
²⁰W. C. Dash and R. Newman, *Phys. Rev.* **99**, 1151 (1955).
²¹G. G. Macfarlane, T. P. McLean, J. E. Quarrington, and V. Roberts, *Phys. Rev.* **108**, 1377 (1957).
²²J. S. Kline, F. H. Pollak, and M. Cardona, *Helv. Phys. Acta* **41**, 968 (1968).
²³G. G. Macfarlane, T. P. McLean, J. E. Quarrington, and V. Roberts, *Phys. Rev.* **111**, 1245 (1958).